



## Additional Erythrocyte Curve Improves the Diagnostic Value of Graphic Type Differentiation of Synovial Cell Count Analytics for Diagnosis of Late Periprosthetic Joint Infection

Marius Hoyka<sup>1</sup>, Florian Hubert Sax<sup>1</sup>, Benedikt Bliersch<sup>1,2</sup>, Elke Weissbarth<sup>1</sup>, Philipp Schuster<sup>1,3</sup>, Irina Berger<sup>4</sup>, Hannsjörg Baum<sup>5</sup>, Bernd Fink<sup>1,6</sup>

### Abstract

**Aim:** The determination of the synovial aspirate cell count is one of the central parameters for diagnosing late periprosthetic joint infection (PJI). A number of different threshold values between 1,100 cells/ $\mu$ L and 5,000 cells/ $\mu$ L have been described, which can be caused by counting of additional abrasion or wear particles using automated cell counters. A new graphic cell distribution charts defined six so-called LMNE matrices (leukocyte-monocyte-neutrophil-eosinophil matrices): abrasion type (type I), infection type (type II), mixed type (type III), indifference type (type IV), haematoma type (type V) and mixed type II (haematoma and infection) (type VI), whereby types I - IV correspond to the histological classification of Morawietz and Krenn. The aim of the study was to evaluate the diagnostic value of the graphical cell type differentiation and the correlation between the LMNE types and the histological types using the new automated cell counter Yumizen H500 and to verify if the new additional erythrocyte curve of this device gives additional helpful information.

**Methods:** Synovial aspirates of 585 knee and 196 hip arthroplasties (410 women, 371 men) were examined by cultivation, alpha-defensin and cell count analysis (using the Yumizen H500 haematology analyser with cell distribution plots (LMNE matrices)) according to the ICM criteria 2018. Periprosthetic tissue obtained from 288 knee prostheses and 116 hip prostheses during revision surgery was analysed microbiologically and histologically using the Morawietz and Krenn classification.

**Results:** The LMNE matrices significantly increased the diagnostic value of the cell count, especially for cell count values < 1500 cells/ $\mu$ L (sensitivity: 96.4-97.3%, specificity: 99.0%). There was a highly significant correlation between the LMNE types I - IV and the histological classification according to Morawietz ( $p < 0.001$  and Cramer's V value of 0.96). The erythrocyte field is helpful to identify leucocytes related to hematoma in the aspirate.

**Conclusion:** The graphical representation of the synovial cell count analysis is a reproducible and helpful method for differentiating between real periprosthetic infections with an increased leukocyte count and false-positive values due to the presence of wear particles with advantages of the new Yumizen H500.

### Affiliation:

<sup>1</sup>Department for Joint Replacement, Rheumatoid and General Orthopaedics, Orthopaedic Clinic Markgröningen, Kurt-Lindemann-Weg 10, 71706 Markgröningen, Germany

<sup>2</sup>Department of Trauma and Reconstructive Surgery, BG Klinik, University of Tübingen, Schnarrenbergstraße 95, 72076 Tübingen, Germany

<sup>3</sup>Department of Orthopedics and Traumatology, Clinic Nuremberg, Paracelsus Medical Private University, Nuremberg, Breslauer Straße 201, 90471 Nürnberg, Germany.

<sup>4</sup>Institute of Pathology, Klinikum Kassel, Mönchebergstraße 41-43, 34125 Kassel, Germany.

<sup>5</sup>Institute for Laboratory Medicine, Orthopaedic Clinic Markgröningen, Kurt-Lindemann-Weg 10, 71706, Markgröningen, Germany.

<sup>6</sup>Orthopaedic Department, University Hospital Hamburg-Eppendorf, Martinistrasse 52, 20251 Hamburg, Germany

### \*Corresponding author:

Bernd Fink, Department for Joint Replacement, Rheumatoid and General Orthopaedics, Orthopaedic Clinic Markgröningen, Kurt-Lindemann-Weg 10, 71706 Markgröningen, Germany.

**E.mail:** bernd.fink@rkh-gesundheit.de

**Citation:** Marius Hoyka, Florian Hubert Sax, Benedikt Bliersch, Elke Weissbarth, Philipp Schuster, Irina Berger, Hannsjörg Baum, Bernd Fink. Additional Erythrocyte Curve Improves the Diagnostic Value of Graphic Type Differentiation of Synovial Cell Count Analytics for Diagnosis of Late Periprosthetic Joint Infection. Journal of Surgery and Research. 8 (2025): 488-500.

**Received:** September 07, 2025

**Accepted:** September 16, 2025

**Published:** October 08, 2025

**Keywords:** Periprosthetic Joint Infection (PJI); Knee Arthroplasty; Hip Arthroplasty; Synovial Cell Count Analysis; LMNE Matrix

## Introduction

Periprosthetic joint infection (PJI) is a devastating complication of total joint arthroplasty with an incidence between 0.85% and 2% for hip and knee replacement [1-3]. It is the third commonest cause (after aseptic loosening and dislocation) of total hip revision surgery and the main cause of total knee revision surgery [4-7]. Diagnosis of late PJI is difficult because systemic inflammatory reactions are mostly missing and no single diagnostic test with an accuracy of 100% exists. However, using a variety of diagnostic tests together has been shown to be beneficial [8-11]. The determination of the leukocyte count (WBC) in the synovial joint fluid represents one of the key diagnostic methods and parameters in PJI diagnosis [12-15]. As one of the minor criteria, it is included in the MSIS criteria, as well as the more recent ICM criteria [16,17]. For several reasons, it is difficult to set the cut-off value of WBC for late/chronic periprosthetic joint infection and, thus, thresholds vary between the different published reports [18]. The thresholds described [13,18] range from 1,100 cells/ $\mu$ L [19] to 5,000 cells/ $\mu$ L [20]. The threshold at which an infection is confirmed has therefore been set at >3,000 cells/ $\mu$ L [21,22], while an infection is considered unlikely at a threshold <1,500 cells/ $\mu$ L [21]. There are different factors leading to this wide variance of thresholds such as the duration of symptoms, the time after the operation, administered antibiotics and detected microorganisms [14,23,24]. Moreover, total hip arthroplasties with metal-on-metal articulations often show levels of WBC in the aspirate above the threshold of 1,500 cells/ $\mu$ L but in the absence of any infection [25,26]. Therefore, not only leukocytes in the aspirate but also abrasion particles may be counted by the automatic cell counter.

In a previous study, we were able to differentiate between leukocytes and wear particles using the automated cell counter ABX Pentra XL 80 (Horiba Medical, Montpellier, France) [18]. Six different so-called LMNE types were described [18,27]. Moreover, we could show that those LMNE types correlate highly significantly (Cramer-V test 0,529) [18] with the equally named histological types I–IV according to Krenn et al. [28,29] and Morawietz [30]. In the meantime, the next generation of automated cell counters - the Yumizen H500 - has been launched on the market. Compared to the ABX Pentra XL 80, however, the LMNE diagrams look different and additional fields for identifying hematoma (that might increase the leucocyte count of the aspirate) exist [27]. We could show that LMNE type differentiation was possible with the new device [27], but the value of this diagnostic tool and the correlation to the histological types has not yet been examined. Therefore, the aim of the current study was to evaluate the diagnostic value of the graphical cell type differentiation and the correlation between the LMNE types and the histological types using the new automated cell counter Yumizen H500 and to verify if the new additional

erythrocyte curve of this device gives additional helpful information.

## Materials and Methods

From January 2022 to November 2024, data of 816 patients with 607 total knee and 209 total hip arthroplasties were prospectively entered into a data system and analyzed retrospectively. All patients underwent preoperative joint aspiration to verify a late periprosthetic joint infection (PJI). Patients with an insufficient amount of aspirate were excluded, resulting in 781 patients with 585 total knee replacements (TKRs) and 196 hip replacements (THRs). The mean age of the patients (410 women and 371 men) was 67 years (SD = 30 years, Range: 37 – 97 years). The synovial aspirates were examined by cultivation and alpha-defensin. Additionally, cell count analysis was performed by the Yumizens H500 (Horiba Medical, Montpellier, France), a laboratory diagnostic device for WBC-differentiation of blood and body fluids. The so-called 5-DIFF processing mode was used providing additional determination of 26 laboratory parameters including the 5 cell types lymphocytes, monocytes, eosinophils, neutrophils and basophils as well as large, immature cells and atypical lymphocytes. The X-axis of the LMNE matrix visually displays the volume difference of the cells as a result of the impedance measurement, while the Y-axis shows the differentiation of the light absorption in flow cytometry (Figure 1) allowing the leukocyte populations to be graphically assigned and, consequently, differentiated. Impurities, known as abrasion or wear particles are depicted in the so-called NOISE area of the LMNE matrix [18,27] (Figure 1).

In cases of elevated cell counts, the counting was repeated manually using a Neubauer improved chamber (Carl Roth GmbH, Karlsruhe, Germany). Synovial fluid was aspirated immediately into pediatric blood culture bottles (779 cases) and incubation was carried out for 14 days according to the

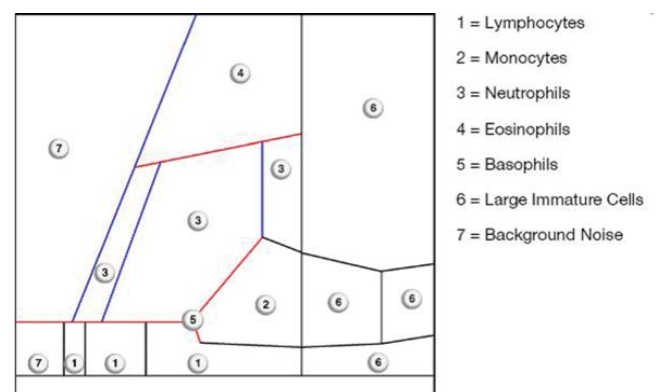


**Figure 1:** LMNE matrix with the different areas corresponding to the leukocyte populations and the NOISE area of the Yumizen H500.

recommendation of Schäfer et al. [31]. The ELISA-Test was used to analyze alpha-defensin in 767 cases whereas serum CRP level was determined in all patients. During the revision surgery of 288 TKRs and 116 THRs (231.5 months (SD = 79.2 months, Range: 1-462 months) after the primary implantation), five samples from the periprosthetic connective tissue membrane and the synovium adjacent to the prosthesis were taken for histological assessment and cultivation [31].

The results were analyzed in accordance with the ICM-criteria [11] and compared with the results of the aspiration. In addition to counting polymorphonuclear leukocytes per high power field, the classification by Morawietz and Krenn [28-30] was used for the histological analysis of the periprosthetic tissue to distinguish between type I – IV. Without knowledge of the associated histology, the evaluations and assignment of the matrices to the different types were independently carried out twice by 2 examiners (MH and BF) with an intrarater intraclass correlation coefficient of 0.99 and of 0.98, respectively.

SPSS for Windows (version 22; IBM Corp.; Armonk, NY) was used for statistical analysis. Nominal variables were compared between groups using the chi-square test, and correlations between nominal variables were analyzed using the Cramer-V test ( $> 0.5$  was considered a strong correlation) by generally setting the level of significance at  $p < 0.05$ . For calculation of the cell count threshold, a receiver operating characteristics curve (ROC-curve) was used. Sensitivity and specificity as well as likelihood ratios were calculated for evaluation of the test performance. All subjects gave their informed consent for inclusion before they participated in the study. The study was conducted in accordance with the Declaration of Helsinki, and the protocol was approved by the Ethics Committee of Landesärztekammer Badenwürttemberg (committee's reference number F-2023-015).

## Results

Seven distinct graphical types could be identified by examining the LMNE matrices of the synovial fluid: type I (abrasion type) in 201 patients (25.7%) (Figure 2), type II (infection type) in 93 patients (11.9%) (Figure 3), type III (mixed type of infection and abrasion) in 20 patients (2.6%) (Figure 4), type IV (indifference type) in 436 patients (55.8%) (Figure 5), type V (hematoma) in 30 patients (3.9%) (Figure 6) and type VI (mixed type of hematoma and infection types) in 1 patient (0.1%) (Figure 7). Two patients with a type I LMNE matrix showed an admixture of hematoma in the aspirate. This constellation had not been described in the previous papers and was classified as abrasion subtype IB (Figure 8), because the abrasion type I could be verified histologically. In cases with elevated cell counts, manual counting with a

Neubauer improved chamber (Carl Roth GmbH, Karlsruhe, Germany) showed lower cell numbers with a difference between manually and automated counts of  $M = 936.4$  cells (SD = 814.7 cells) for the type I and  $M = 9,454.0$  cells (SD = 13,875.7 cells) for the type III aspirates.

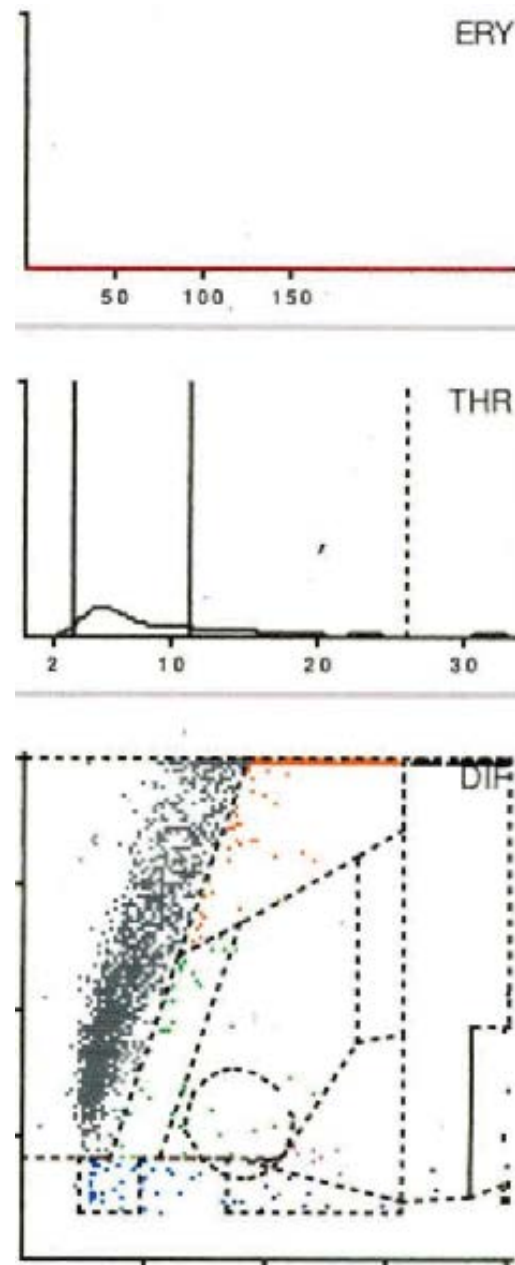


**Figure 2:** LMNE matrix of a type I (abrasion type) with a cloud in the NOISE-area of a 79-year-old female patient with an aspirate of the knee arthroplasty 12 years postoperative. Clusters of data points inside as well as at the border to the NOISE area of the LMNE matrix were classified as wear particles since they could not be assigned to any particular cell type. The measured cell count was 2150 cells/ $\mu$ L, 23.4 % PMN (polymorphonuclear leucocytes), CRP = 9 mg/L, alphadefensin = 0.1, histology = Krenn Type I, microbiological cultivation = negative.

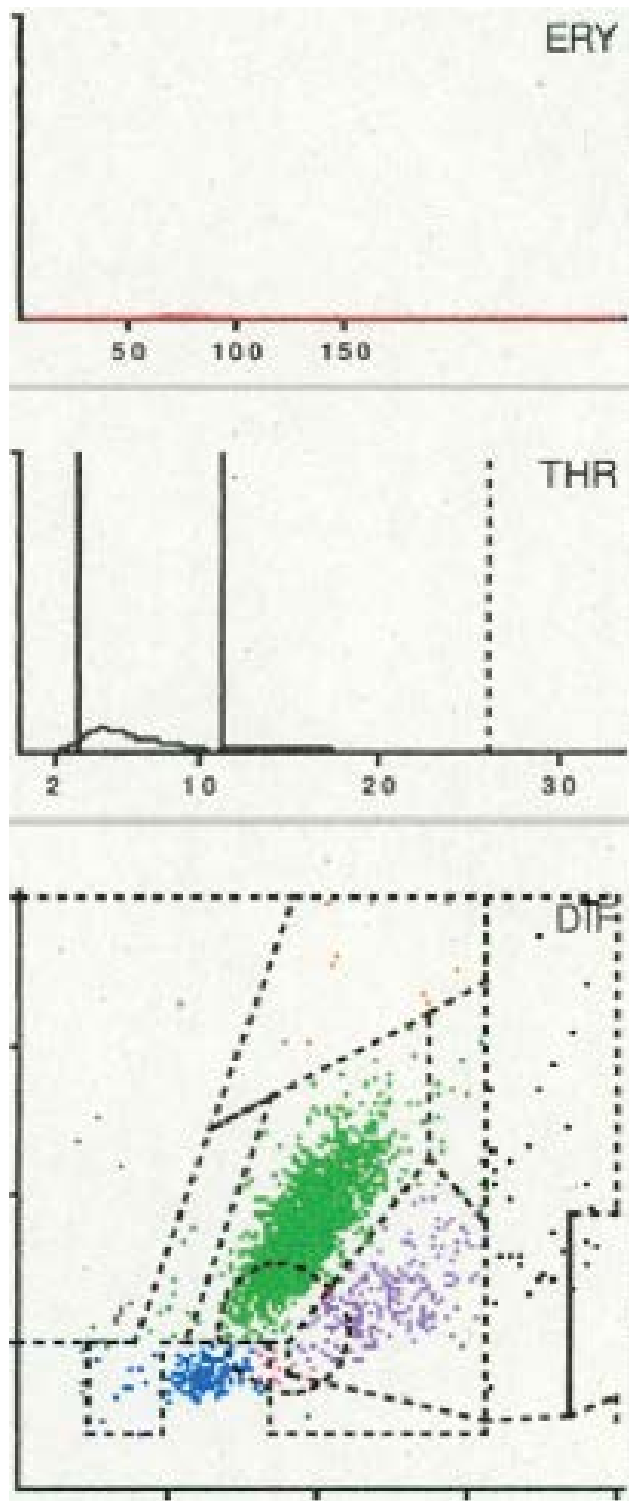


**Figure 3:** LMNE matrix of a type II (infection type) represented by a cluster of data points that corresponds to the location of neutrophil leukocytes in the graphical representation in a 75-year-old female patient with a late periprosthetic joint infection of a total knee arthroplasty. The measured cell count was 4490 cells/ $\mu$ L, 85.5 % PMN, CRP = 8.9 mg/L, alphadefensin = 0.9, histology = Krenn Type II, microbiological cultivation = *Cutibacterium agnes*.

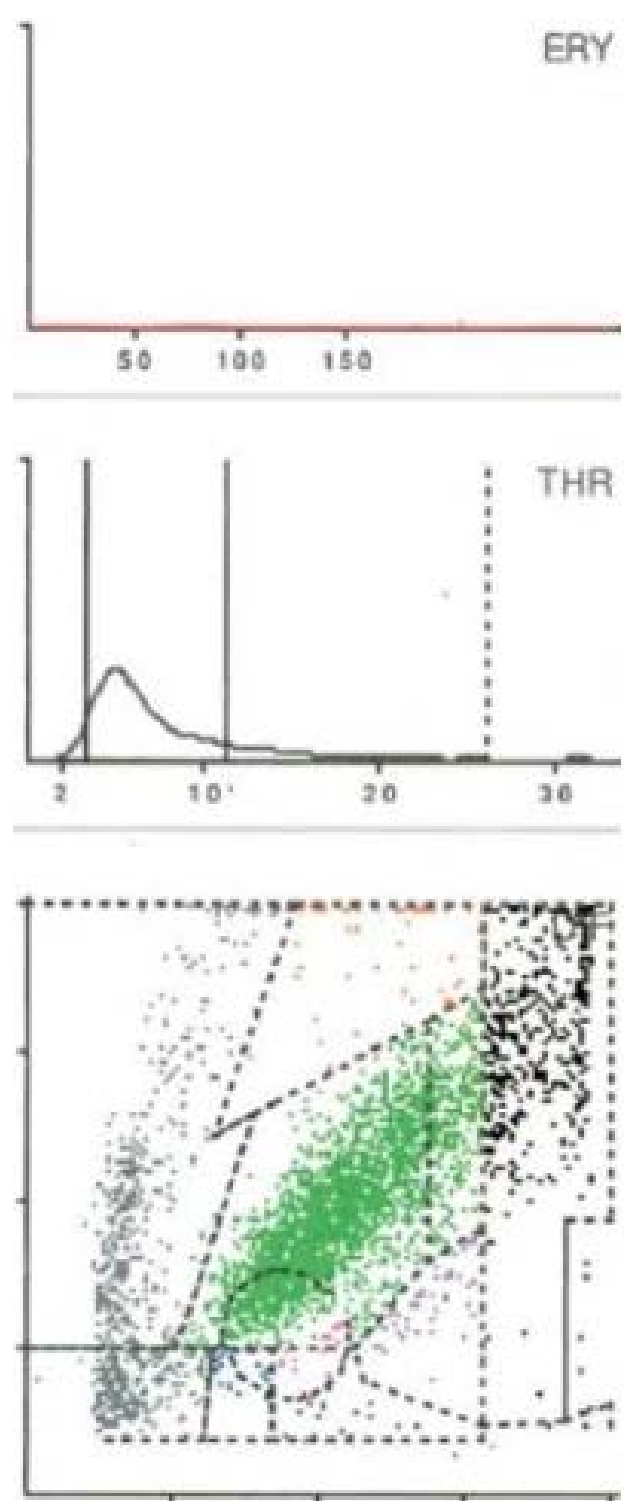


**Figure 4:** LMNE matrix of a type III (combined type) with one cloud in the area of the neutrophil leukocytes and a second cloud in the NOISE area in a 63-year-old female patient with a periprosthetic joint infection of a total hip arthroplasty. The measured cell count was 2940 cells/ $\mu$ L, 48.3 % PMN, CRP = 33.7 mg/L, alphadefensin = 1.4, histology = Krenn Type II, microbiological cultivation = *Staphylococcus hominis*.



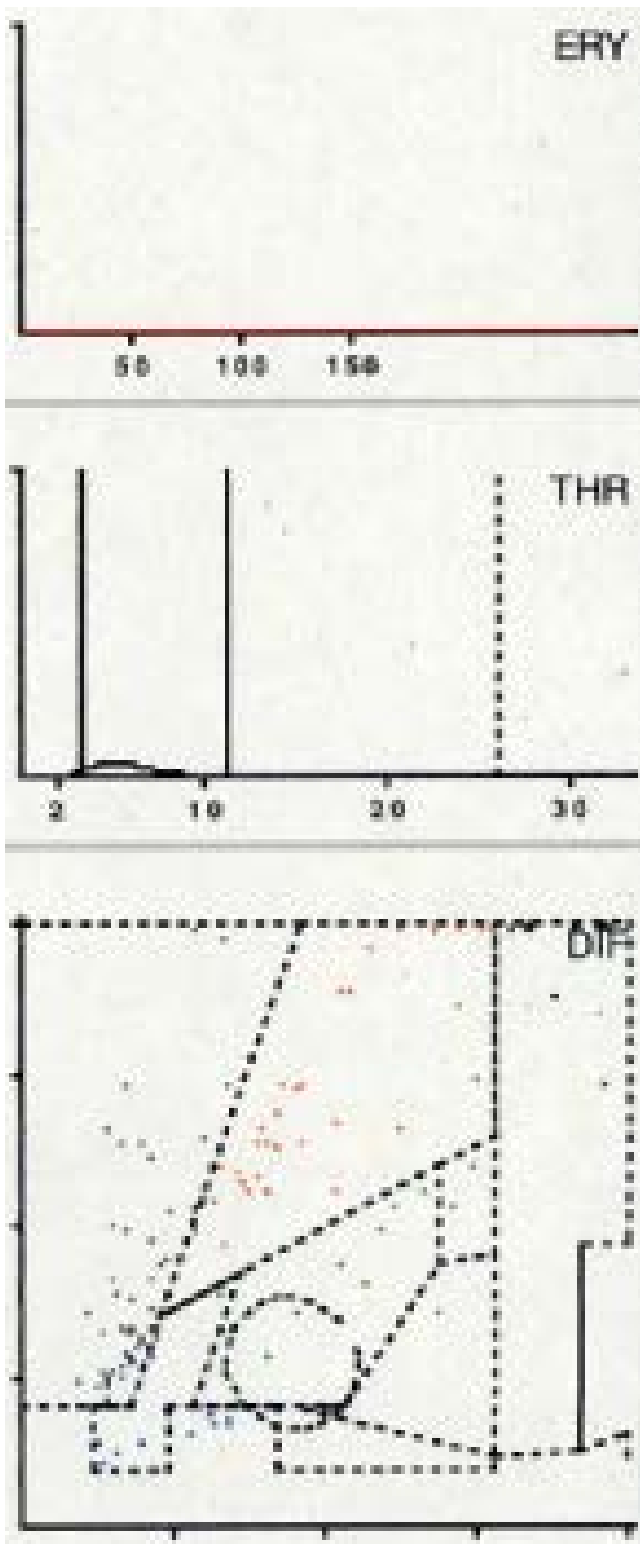


**Figure 5:** LMNE matrix of a type IV (indifference type) with no clear differentiation in cell types or particles in a 62-year-old male patient with a total knee arthroplasty. The measured cell count was 830 cells/ $\mu$ L, 30.3 % PMN, CRP = 7.2 mg/L, alphadefensin = 0.1, histology = Krenn Type IV, microbiological cultivation = negative.

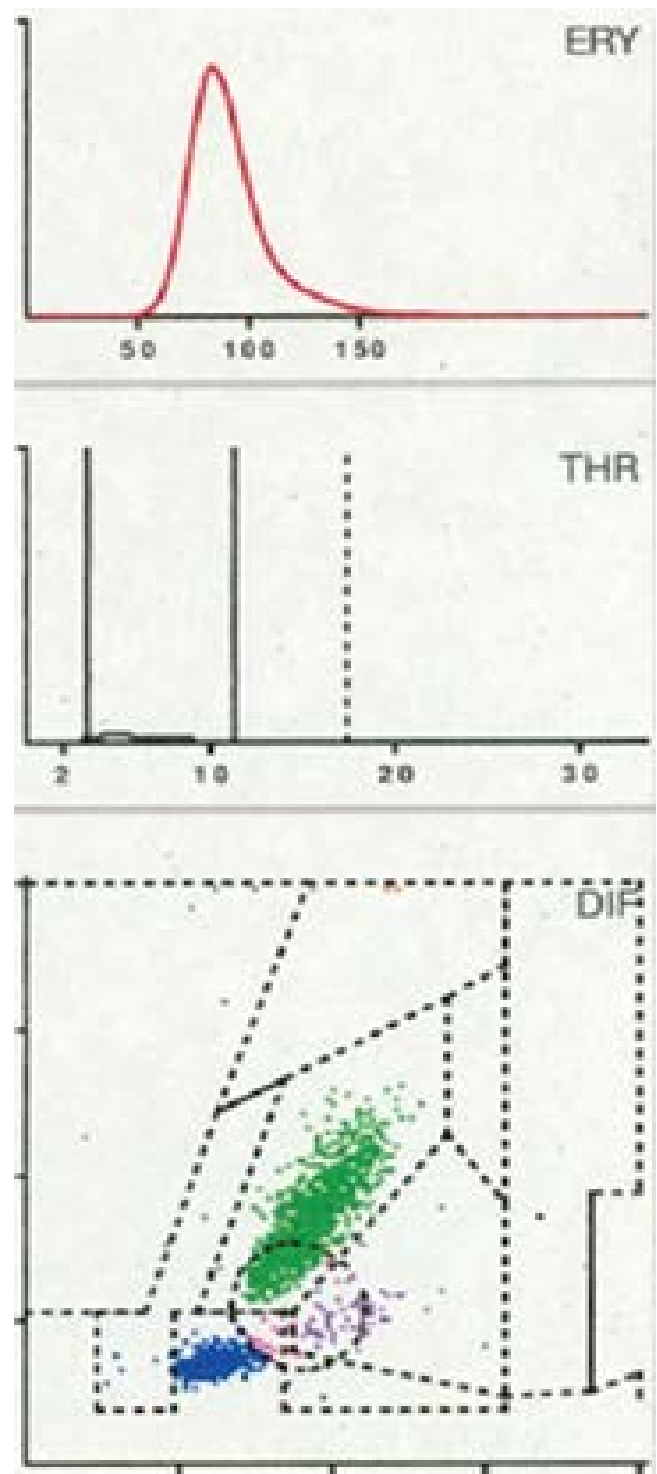


**Figure 6:** LMNE matrix of a type V (hematoma) in a 65-year-old female patient with a hematoma 6 months after hip arthroplasty with a dislocation. There is a cluster in the field of the lymphocytes, monocytes and another clear cluster in the field of the neutrophils as well as a peak in the erythrocyte field. The measured cell count was 3,050 cells/ $\mu$ L with 68,9 % PMN, CRP = 9.2 mg/L, alphadefensin = < 0.1, histology = Krenn Type IV, microbiological cultivation = negative.

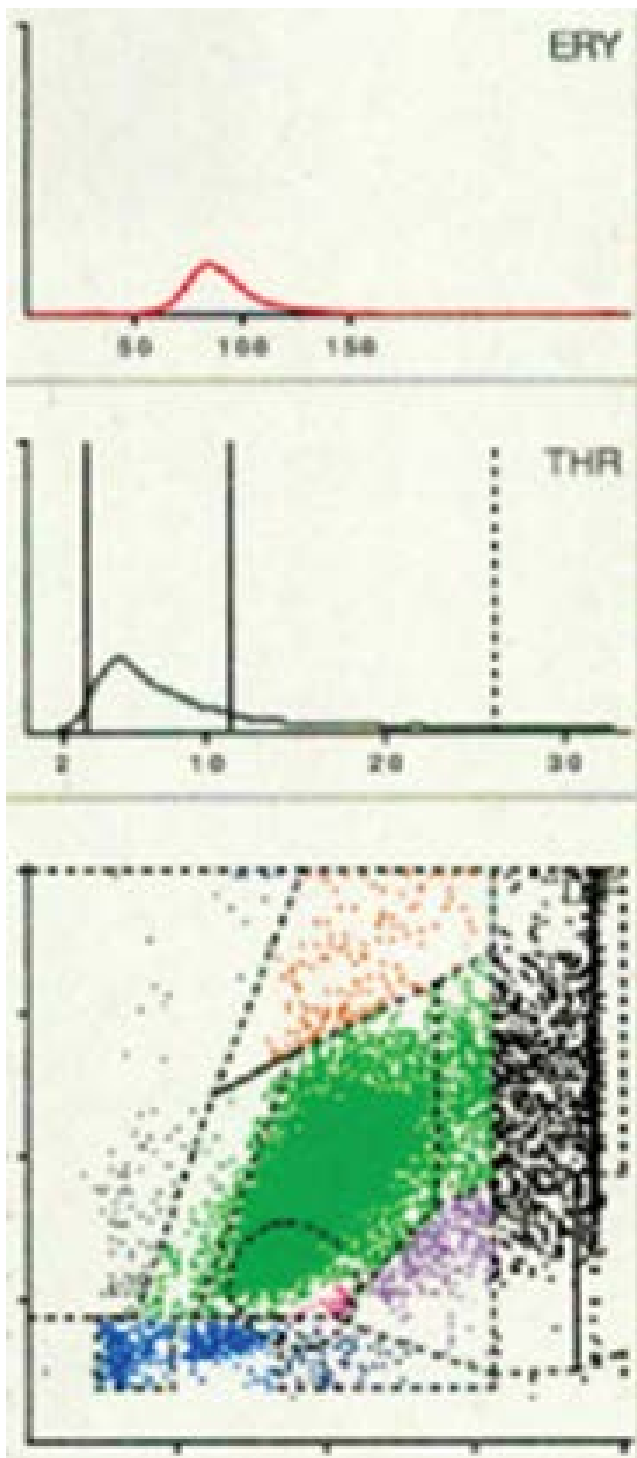


**Figure 7:** LMNE matrix of a type VI (combined infection and hematoma) 5 years after implantation of a hip arthroplasty and 2 weeks of severe pain in a 73-year-old male patient. There is a large cluster in the area of the neutrophil leukocytes and increases in the other areas of the white blood cells as well as a peak in the erythrocyte field. The measured cell count was 42,060 cells/ $\mu$ L with 87.7% PMN, CRP of 39 mg/L, alphadefensin = 6.0, histology = Krenn Type II, microbiological cultivation = *Cutibacterium agnes*.

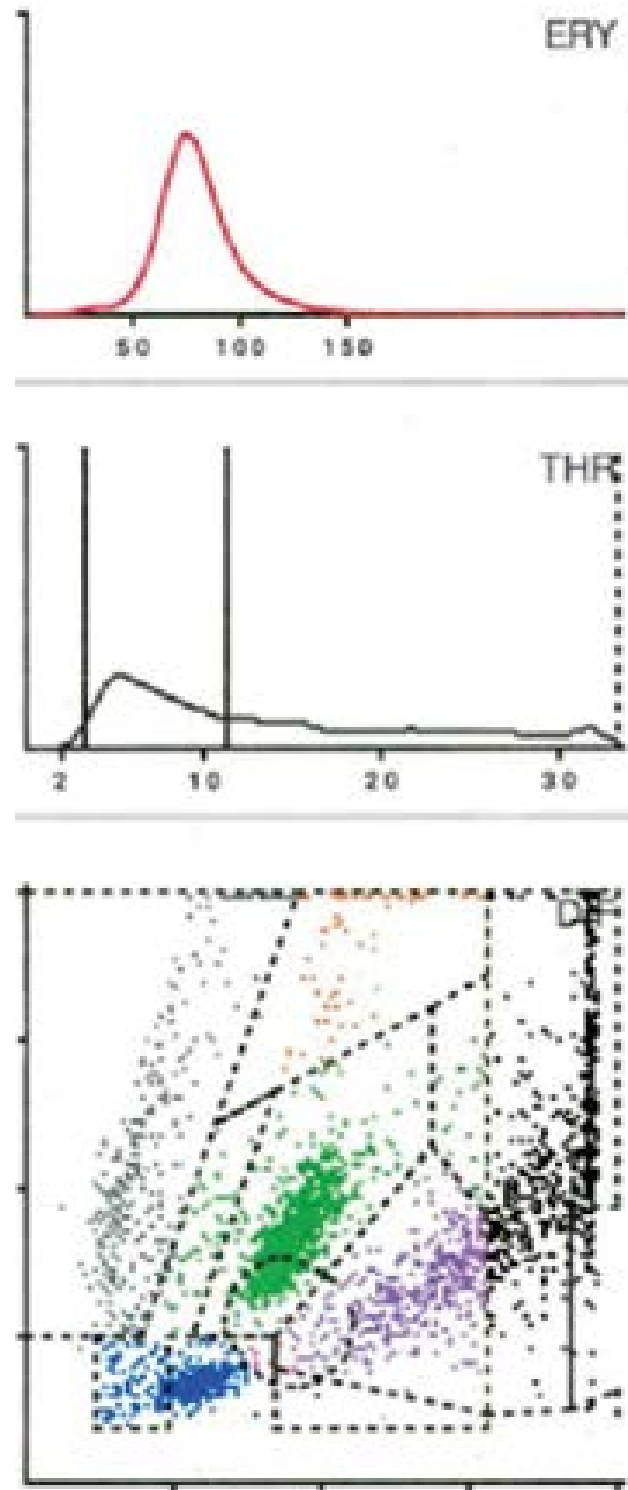


**Figure 8:** LMNE matrix of a type IB (abrasion type + hematoma) of a 71-year-old male patient with an aspirate of the knee arthroplasty 8 years postoperative. An admixture of hematoma in the aspirate is represented by clusters in the fields for eosinophils, monocytes, lymphocytes and neutrophils and additionally by the peak in the erythrocyte curve [6]. The measured cell count was 4,790 cells/ $\mu$ L, 38.0 % PMN, CRP = 3.6 mg/L, alphadefensin = 0.1, histology = Krenn Type I, microbiological cultivation = negative.

**Table 1:** Distribution of the patients according to the four different LMNE matrices and the histological types described by Morawietz and Krenn [28-30].

LMNE Type	Histological Classification				
	Type I	Type II	Type III	Type IV	Total
LMNE Type I	115	0	0	4	119
LMNE Type IB	2	0	0	0	2
LMNE Type II	1	77	0	0	78
LMNE Type III	0	1	17	0	18
LMNE Type IV	21	2	0	158	181
LMNE Type V	6	0	0	0	6
LMNE Type VI	0	0	0	0	0
Total	145	80	17	162	404

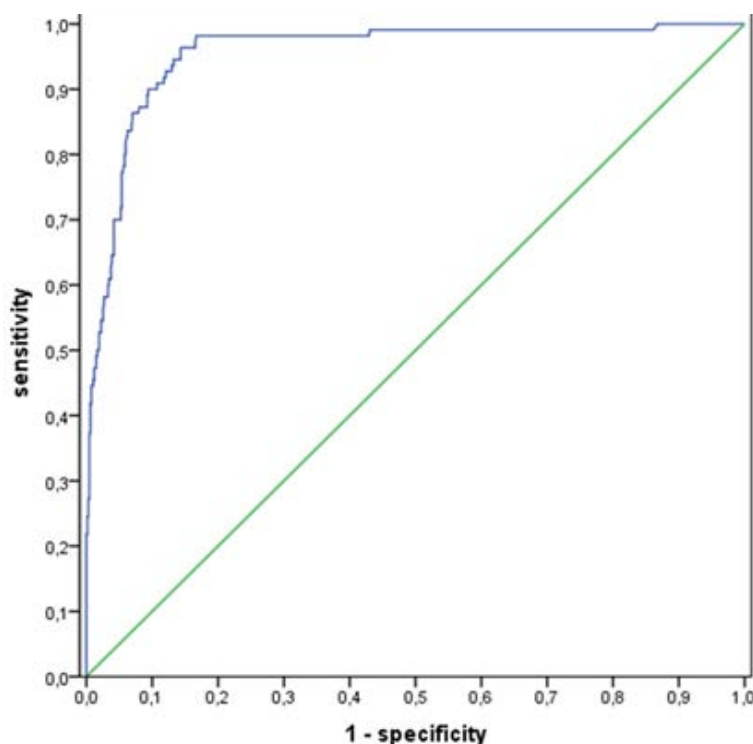


**Figure 9:** Receiver operating characteristics curve (ROC-curve) with the calculation of the threshold of cell count at a value of 2500 cells/ $\mu$ L with a sensitivity of 93.6 % and a specificity of 99.0 %. Area under the curve = 0.956.

According to the ICM criteria, 110 patients (14.1%) had an infection [11]. 114 aspirates (14.6%) were associated with an infection (type II, III or VI) in the LMNE matrix analysis. There was a highly significant correlation between the evaluation of the LMNE matrices and the histological classification according to Morawietz and Krenn [29-31] ( $p < 0.001$  and Cramer test V value of 0.96) (Table 1).

The additional evaluation of the LMNE matrices significantly increased the diagnostic value of the cell count, especially for cell count values  $< 1,500$  cells/ $\mu$ L (sensitivity: 96.4-97.3%, specificity: 99.0%) (Table 2A, 2B).

Table 2A shows the diagnostic value of the cell count at different thresholds combined with the LMNE infection types II, III and VI taking into account the ICM criteria [11] and table 2B without consideration of the LMNE-infection types. The threshold value of the WBC count could be set lower without loosening the specificity by taking into account the diagnostic significance of the LMNE matrix as well (Table 2A). The calculation of the cell count threshold without the LMNE-types using the receiver operating characteristic curve analysis resulted in a cut-off of 2,500 cells/ $\mu$ L at a sensitivity of 93.6 % and a specificity of 99.0 % (Figure 9). The value of the other parameters are listed in table 3.

**Table 2A:** Diagnostic value of the cell count at different thresholds (X) combined with the LMNE Type 2, 3 and 6 (PJI); PPV = Positive Predictive Value, NPV = Negative Predictive Value.

							LR +	LR -
		Infection			Accuracy	98.70%	93.24	0.03
		yes	no		Sensitivity	97.30%		
X = 500 cells/ $\mu$ L	pos.	107	7	114	Specificity	99.00%		
+ LMNE	neg.	3	664	667	PPW	93.90%		
Type II/III/VI		110	671	781	NPW	99.60%		
		Infection			Accuracy	98.60%	92.37	0.04
		yes	no		Sensitivity	96.40%		
X = 1000 cells/ $\mu$ L	pos.	106	7	113	Specificity	99.00%		
+ LMNE	neg.	4	664	668	PPW	93.80%		
Type II/III/VI		110	671	781	NPW	99.40%		
		Infection			Accuracy	98.60%	92.37	0.04
		yes	no		Sensitivity	96.40%		
X = 1500 cells/ $\mu$ L	pos.	106	7	113	Specificity	99.00%		
+ LMNE	neg.	4	664	668	PPW	93.80%		
Type II/III/VI		110	671	781	NPW	99.40%		
		Infection			Accuracy	98.20%	89.76	0.06
		yes	no		Sensitivity	93.60%		
X = 2000 cells/ $\mu$ L	pos.	103	7	110	Specificity	99.00%		
+ LMNE	neg.	7	664	671	PPW	93.60%		
Type II/III/VI		110	671	781	NPW	99.00%		
		Infection			Accuracy	97.70%	86.27	0.1
		yes	no		Sensitivity	90.00%		
X = 2500 cells/ $\mu$ L	pos.	99	7	106	Specificity	99.00%		
+ LMNE	neg.	11	664	675	PPW	93.40%		
Type II/III/VI		110	671	781	NPW	98.40%		
		Infection			Accuracy	97.70%	118.34	0.12
		yes	no		Sensitivity	88.20%		
X = 3000 cells/ $\mu$ L	pos.	97	5	102	Specificity	99.30%		
+ LMNE	neg.	13	666	679	PPW	95.10%		
Type II/III/VI		110	671	781	NPW	98.10%		



**Table 2B:** Diagnostic value of the cell count at different thresholds (X); PPV = Positive Predictive Value, NPV = Negative Predictive Value.

							LR +	LR -
		Infection			Accuracy	41.20%	1.45	0.03
		yes	no		Sensitivity	99.10%		
X = 500 cells/ $\mu$ L	pos.	109	458	567	Specificity	31.70%		
	neg.	1	213	214	PPW	19.20%		
		110	671	781	NPW	99.50%		
		Infection			Accuracy	71.20%	2.95	0.03
		yes	no		Sensitivity	98.20%		
X = 1000 cells/ $\mu$ L	pos.	108	223	331	Specificity	66.80%		
	neg.	2	448	450	PPW	32.60%		
		110	671	781	NPW	99.60%		
		Infection			Accuracy	82.10%	4.77	0.02
		yes	no		Sensitivity	98.20%		
X = 1500 cells/ $\mu$ L	pos.	108	138	246	Specificity	79.40%		
	neg.	2	533	535	PPW	43.90%		
		110	671	781	NPW	99.6		
		Infection			Accuracy	86.80%	6.53	0.04
		yes	no		Sensitivity	96.40%		
X = 2000 cells/ $\mu$ L	pos.	106	99	205	Specificity	85.20%		
	neg.	4	572	576	PPW	51.70%		
		110	671	781	NPW	99.30%		
		Infection			Accuracy	88.60%	7.7	0.09
		yes	no		Sensitivity	91.80%		
X = 2500 cells/ $\mu$ L	pos.	101	80	181	Specificity	88.10%		
	neg.	9	591	600	PPW	55.80%		
		110	671	781	NPW	98.50%		
		Infection			Accuracy	90.50%	9.64	0.12
		yes	no		Sensitivity	89.10%		
X = 3000 cells/ $\mu$ L	pos.	98	62	160	Specificity	90.80%		
	neg.	12	609	621	PPW	61.30%		
		110	671	781	NPW	98.10%		

**Table 3:** Diagnostic value of other parameters; PPV = Positive Predictive Value, NPV = Negative Predictive Value.

							LR +	LR -
		Infection			Accuracy	98.70%	93.24	0.03
		yes	no		Sensitivity	97.30%		
LMNE type	pos.	107	7	114	Specificity	99.00%		
II/III/VI	neg.	3	664	667	PPW	93.90%		
		110	671	781	NPW	99.60%		
		Infection			Accuracy	78.20%	3.49	0.38
		yes	no		Sensitivity	69.90%		
CRP > 10 mg/dl	pos.	95	129	224	Specificity	80.00%		
	neg.	41	516	557	PPW	42.40%		
		136	645	781	NPW	92.60%		
		Infection			Accuracy	91.90%	13.27	0.22
		yes	no		Sensitivity	79.10%		
PMN > 65%	pos.	87	40	127	Specificity	94.00%		
	neg.	23	631	654	PPW	68.50%		
		110	671	781	NPW	96.50%		
		Infection			Accuracy	92.10%	30.5	0.46
		yes	no		Sensitivity	54.50%		
PMN > 80%	pos.	60	12	72	Specificity	98.20%		
	neg.	50	659	709	PPW	83.30%		
		110	671	781	NPW	92.90%		
		Infection			Accuracy	97.40%	279.76	0.16
		yes	no		Sensitivity	83.60%		
Microbiology	pos.	92	2	94	Specificity	99.70%		
Aspirate	neg.	18	667	685	PPW	97.90%		
		110	669	779	NPW	97.40%		
		Infection			Accuracy	93.60%	27.4	0.3
		yes	no		Sensitivity	70.90%		
Alpha-Defensin	pos.	78	17	95	Specificity	97.40%		
(≥1)	neg.	32	640	672	PPW	82.10%		
		110	657	767	NPW	95.20%		
		Infection			Accuracy	98.00%	60.19	0.03
		yes	no		Sensitivity	96.80%		
Histology	pos.	90	5	95	Specificity	98.40%		
(≥ 5 PMN in 5 high	neg.	3	306	309	PPW	94.70%		
power fields)		93	311	404	NPW	99.00%		

## Discussion

The determination of the leukocyte count (WBC) in the synovial joint fluid represents one of the key diagnostic methods and parameters in PJI diagnostics [18,19,27]. False positive deviations of synovial leukocyte counts can be caused by abrasion particles (polyethylene or metal particles) originating from the articular surface of the artificial joint [18]. The graphic type differentiation of synovial cell count data into so-called LMNE matrices has already been proven to be a helpful diagnostic method for the diagnosis of late periprosthetic joint infections to differentiate between falsely raised cell counts due to abrasion particles and raised numbers of leukocytes due to real periprosthetic joint infection [18]. The differentiation of the LMNE matrices into the LMNE types I to VI with the ABX Pentra XL 80 (Horiba Medical, Montpellier, France) could clearly be reproduced with the new generation of this laboratory diagnostic device, the Yumizen H500 (Horiba Medical, Montpellier, France) [27]. However, the value of this diagnostic tool and the correlation with the histological types of Morawietz and Krenn [28-30] have not yet been proven. The additional evaluation of the LMNE matrices (type II, III and VI) shows a high sensitivity (88.2-97.3%) and specificity (99.0-99.3%) for the diagnosis of late periprosthetic infections. In comparison to an isolated cell count analysis (sensitivity 89.1-99.1%, specificity 31.7-90.8%), it increased the diagnostic value significantly, especially for cell count values <1,500 cells/ $\mu$ L (sensitivity: 96.4-97.3%, specificity: 99.0%). Due to the combined analysis of cell count and LMNE types II, III, or VI, the cut-off value of the cell count in the aspirate could be lowered without losing specificity. Moreover, there was a significant level of agreement between the four distribution types in the LMNE matrix analysis by the cell counter Yumizen H500 and the four histopathological types described by Morawietz and Krenn [28-30]. The correlation was even better with the new device Yumizen H500 compared to the previous device ABX Pentra XL (Cramer-value 0.96 compared to 0.526) [18]. An explanation for this can be the additional erythrocyte field of the new device which helps to identify additional blood in the aspirate (which can increase the leukocyte count).

The differentiation of infection-related leukocytes and abrasion particles by the LMNE matrices is especially helpful when metal abrasion particles are present in joint aspirates, because these aspirates can be associated with apparently very high cell counts as well as exhibiting elevated CRP and alpha-defensin values [32]. Moreover, Karlidag et al. [28] found that polyethylene wear can result in cell counts in aseptic revisions being above the threshold of 1,500 cells/ $\mu$ L, where PJI would be classified as likely [21]. In the absence of a graphical representation of the cell count data, these features could be incorrectly interpreted as a periprosthetic infection. Distinguishing leukocytes and wear particles in the aspirate is

also possible by manual counting using a microscope. In turn, this procedure has been shown to result in an inter-observer variance of more than 20% reducing the accuracy of manual counting of WBC in synovial fluid compared to automated counting [33]. Therefore, compared to the traditional manual alternative, the improved automatic counting process described here appears to be a more promising technique.

This study has some limitations. First, such an LMNE matrix of the synovial aspirate cannot be created by all cell counting devices. For creating the LMNE matrix, measurement of the light absorption of the cells or particles is required, while many cell counting devices only measure the scattered light and the size of the cells or particles. Second, unlike the Yumizen H500, not every automated cell counter has an additional erythrocyte field that can identify blood contamination of the aspirate and, as a result, interpret a portion of the observed cell count as leukocytes from the aspirate's blood. If automated cell counters do not provide this additional information, the presence of blood may reduce the usefulness of the aspirate cell count. Third, both the LMNE Matrix and histopathology's type classifications are somewhat dependent on the personal interpretation and experience of the examiner. A certain subjectivity in the interpretation of the LMNE matrices cannot be ruled out, even though the reliability of this type categorization was extremely high in our investigation. The number of patients was high enough to allow significant correlations to be statistically recognized as such.

## Conclusions

The graphic representation of the cell count analysis of synovial aspirates from joints with endoprostheses is a new and helpful method for diagnosing true periprosthetic infections. The diagnostic value of the cell count analysis will be increased by using a device that visually displays an elevated leukocyte count and detects wear particles that would otherwise lead to an inaccurate interpretation of the data with advantages of the new device Yumizen H500 (additional erythrocyte field). Hereby, as a result of the combination of cell counting and the graphical representation in the LMNE matrix, fewer periprosthetic infections will be overlooked, and the diagnostic value of the cell count analysis in the joint aspirate is increased. Therefore, we believe that this technology should be included in the diagnostic armamentarium of the orthopedic specialist when dealing with loosened or painful endoprostheses.

## Conflict of interest

The authors declare no conflict of interest. The publication fee was paid by Horiba Medical, Montpellier, France.

All authors have read and agreed to the published version of the manuscript.

## Abbreviations

CRP	C-reactive Protein
ICM	International Consensus on Musculoskeletal Infection
LMNE	Leucocyte-Monocyte-Neutrophil-Eosinophil
MSIS	Musculoskeletal Infection Society
PJI	Periprosthetic Joint Infection
PMN	Polymorphonuclear Leucocytes
THR	Total Hip Replacement
TKR	Total Knee Replacement
WBC	White Blood Cell

## References

1. Australian Orthopaedic Association National Joint Replacement Registry (AOANJRR). Hip, Knee & Shoulder Arthroplasty: 2021 Annual Report, Adelaide; AOA, (2021): 1-432.
2. Matar HE, Bloch BV, Snape SE, James PJ. Outcomes of single- and two-stage revision total knee arthroplasty for chronic periprosthetic joint infection. *Bone Jt. J.* 103 (2021): 1373-1379.
3. Springer BD, Etkin CD. The American joint replacement registry and arthroplasty today. *Arthroplasty Today* 2 (2016): 43.
4. Lum ZC, Natsuhara KM, Shelton TJ, et al. Mortality During Total Knee Periprosthetic Joint Infection. *J. Arthroplasty* 33 (2018): 3783-3788.
5. Natsuhara KM, Shelton TJ, Meehan JP, et al. Mortality During Total Hip Periprosthetic Joint Infection. *J Arthroplasty* 34 (2018); 337-S342.
6. Otto-Lambertz C, Yagdiran A, Wallscheid F, et al. Periprosthetic infection in joint replacement. *Dtsch Arztebl Int* 114 (2017): 347-353.
7. Porrino J, Wang A, Moats A, et al. Prosthetic joint infections: diagnosis, management, and complications of the two-stage replacement arthroplasty. *Skeletal Radiol* 49 (2020): 847-859.
8. Fink B, Makowiak C, Fuerst M, et al. The value of synovial biopsy, joint aspiration and C-reactive protein in the diagnosis of late peri-prosthetic infection of total knee replacements. *J Bone Joint Surg Br* 90 (2008): 874-878.
9. Fink B, Gebhard A, Fuerst M, et al. High diagnostic value of synovial biopsy in periprosthetic joint infection of the hip. *Clin Orthop Relat Res* 471 (2013): 956-964.
10. Fink B, Schuster P, Braun R, et al. The diagnostic value of routine preliminary biopsy in diagnosing late prosthetic joint infection after hip and knee arthroplasty. *Bone Joint J* 102 (2020): 329-335.
11. Parvizi J, Tan TL, Goswami K. The 2018 Definition of Periprosthetic Hip and Knee Infection: An Evidence-Based and Validated Criteria. *J Arthroplasty* 33 (2018): 1309-1314.
12. Della Valle CJ, Sporer SM, Jacobs JJ, et al. Perioperative testing for sepsis before revision total knee arthroplasty. *J Arthroplasty* 22 (2007): 90-93.
13. Jandl N, Kleiss S, Mussawy, et al. Absolute synovial polymorphonuclear neutrophil cell count as a biomarker of periprosthetic joint infection. *Bone Joint J* 373 (2023): 381.
14. Trampuz A, Hanssen AD, Osmon DR, et al. Synovial fluid leukocyte count and differential for the diagnosis of periprosthetic knee infection. *Am J Med* 117 (2004): 556-562.
15. Trampuz A, Hanssen AD, Osmon DR, et al. Synovial fluid leukocyte count and differential for the diagnosis of prosthetic knee infection. *The American journal of medicine* 117 (2004): 556-562.
16. Parvizi J, Zmistowski B, Berbari EF et al. New definition for periprosthetic joint infection: from the Workgroup of the Musculoskeletal Infection Society. *Clin Orthop Relat Res* 469 (2011): 2992-2994.
17. Workgroup Convened by the Musculoskeletal Infection Society. New definition for periprosthetic joint infection. *J Arthroplasty* 26 (2011): 1136-1138.
18. Fink B, Hoyka M, Weissbarth E, et al. The Graphical Representation of Cell Count Representation: A New Procedure for the Diagnosis of Periprosthetic Joint Infections. *Antibiotics (Basel)* 10 (2021): 346.
19. Ghanem E, Parvizi J, Burnett RS et al. Cell count and differential of aspirated fluid in the diagnosis of infection at the site of total knee arthroplasty. *J Bone Joint Surg Am* 90 (2008): 1637-1643.
20. Spanghehl MJ, Masri BA, O'Connell JX, et al. Prospective analysis of preoperative and intraoperative investigations for the diagnosis of infection at the sites of two hundred and two total hip arthroplasties. *J Bone Joint Surg Am* 81 (1999): 672-683.
21. McNally M, Sousa R, Wouthuyzen-Bakker M et al. The EBJIS definition of periprosthetic joint infection. A practical guide for clinicians. *Bone Joint J* 103 (2021): 18-25.
22. Parvizi J, Gehrke T. International Consensus Group on Periprosthetic Joint Infection. Definition of periprosthetic joint infection. *J Arthroplasty* 29 (2014): 13-31.
23. Choi HR, Agrawal K, Bedair H. The diagnostic thresholds for synovial fluid analysis in late periprosthetic infection

- of the hip depend on the duration of symptoms. *Bone Joint J* 98 (2016): 1355-1359.
24. Shahi A, Deirmengian CHC, Chen A, et al. Premature Therapeutic Antimicrobial Treatments Can Compromise the Diagnosis of Late Periprosthetic Joint Infection. *Clin Orthop Relat Res* 473 (2015): 2244-2249.
  25. Johnson AH, Brennan JC, Turcotte JJ, et al. Evaluating the diagnostic utility of serum laboratory studies and synovial fluid analysis in identifying periprosthetic joint infection in metal hip revisions. *Cureus* 16 (2024): e70823
  26. Karlidag T, Zann L, Traverso G, et al. Assessing the reliability of automated cell count analysis of synovial fluid in the setting of revision total knee arthroplasty. *Arch Orthop Trauma Surg* 145 (2024): 25.
  27. Fink B, Hoyka M, Blersch BP, et al. Graphic type differentiation of cell count data for diagnosis of early and late periprosthetic joint infection: A new method. *Technol Health Care* 11 (2023): 1-12.
  28. Krenn V, Otto M, Morawietz L, et al. Histopathologic diagnostics in endoprosthetics: Periprosthetic neosynovialitis, hypersensitivity reaction, and arthrofibrosis. *Orthopäde* 38 (2009): 520-530.
  29. Krenn V, Morawietz L, Perino G, et al. Revised histopathological consensus classification of joint implant related pathology. *Pathol Res Pract* 210 (2014): 779-786.
  30. Müller M, Morawietz L, Hasart O, et al. Histopathological diagnosis of periprosthetic joint infection following total hip arthroplasty: use of a standardized classification system of the periprosthetic interface membrane. *Orthopäde* 38 (2009): 1087-1096.
  31. Schäfer P, Fink B, Sandow D, et al. Prolonged bacterial culture to identify late periprosthetic joint infection: A promising strategy. *Clin Inf Dis* 47 (2008): 1403-1409.
  32. Wyles CC, Larson DR, Houdek MT, et al. Utility of synovial fluid aspirations in failed metal-on-metal total hip arthroplasty. *J Arthroplasty* 28 (2013): 818-823.
  33. De Jonge R, Brouwer R, Smit M, et al. Automated counting of white blood cells in synovial fluid. *Rheumatology (Oxford)* 43 (2004): 170-173.



This article is an open access article distributed under the terms and conditions of the [Creative Commons Attribution \(CC-BY\) license 4.0](https://creativecommons.org/licenses/by/4.0/)